

## Novel Coordination Polymers Based on the Tetrathioterephthalate Dianion as the Bridging Ligand

Eleftheria Neofotistou,<sup>†</sup> Christos D. Malliakas,<sup>‡</sup> and Pantelis N. Trikalitis\*<sup>†</sup>

Department of Chemistry, University of Crete, Voutes 71003, Heraklion Crete, Greece, and  
Department of Chemistry, Northwestern University, Evanston, Illinois 60208-3113

Received July 16, 2007

The first examples of coordination polymers based on the tetrathioterephthalate dianion as the bridging ligand are reported. Two novel compounds,  $[M(S_2CC_6H_4CS_2)(DMF)_2](DMF)$  ( $M = Zn, Mn$ ; DMF = dimethylformamide), have been synthesized, and their structural and optical properties were investigated.

Coordination polymers are an important class of functional solids in which strong coordinative chemical bonds between metal centers and organic bridging ligands exist at least in one dimension.<sup>1,2</sup> Although they have a long history, currently there is enormous research activity in the design and synthesis of porous coordination polymers for potential application primarily in the field of gas storage and catalysis.<sup>1,3</sup> In addition to these efforts, there is a steadily increasing interest for the development of metal–organic solids with interesting optoelectronic properties and, in particular, with semiconductive or conductive behavior.<sup>4</sup> For example, the development of three-dimensional (3D) metal–organic networks that combine accessible porosity with useful electronic properties similar to those found in pure inorganic chalcogenide-based materials is highly desirable. The lack of these properties in the overwhelming majority of coordination

polymers is the result of the low electroactivity of the organic bridging units and their weak electronic coupling with metal centers.<sup>4a</sup> The donor atoms are usually hard, such as O or N, resulting in strong electronic barriers between the metal centers and the rest of the organic molecule. Therefore, the proper selection or design of the organic ligand is a key element, and in accordance with the above considerations, examples based on aromatic multifunctional ligands with chalcogenide donor atoms, such as S, have been reported.<sup>5</sup>

Our approach involves the use of chalcogenide-substituted aromatic polycarboxylate-based ligands, such as the tetrathioterephthalate dianion ( $ttp^{2-}$ ). The parent terephthalate dianion (1,4-benzenedicarboxylate, BDC) is a robust bridging ligand that has been used extensively for the construction of important porous metal–organic frameworks (MOFs).<sup>6</sup> In terms of electronic properties, the substitution of O by S decreases the lowest unoccupied molecular orbital (LUMO) energy of the ligand because C–S  $\pi$  bonds are weaker than C–O  $\pi$  bonds and also increases the highest occupied molecular orbital (HOMO) energy because S is less electronegative than O.<sup>7</sup> The decrease in the HOMO–LUMO gap may lead to enhanced electronic communication between the ligand and metal centers. Therefore, the synthesis and characterization of new coordination polymers based on the  $ttp^{2-}$  dianion is highly attractive because it may open the pathway to a novel class of optoelectronically active, multifunctional metal–organic materials.

Herein, we report for the first time that  $ttp^{2-}$  anions are readily combine with  $Zn^{2+}$  in dimethylformamide (DMF) to form an insoluble, dark-red crystalline solid with a chemical formula  $[Zn(S_2CC_6H_4CS_2)(DMF)_2](DMF)$  (**1**). X-ray single-crystal analysis<sup>8</sup> revealed that **1** consists of one-dimensional (1D) zigzag  $[Zn(S_2CC_6H_4CS_2)(DMF)_2]$  chains and free DMF molecules, as shown in Figure 1a. The Zn atom in **1** has a highly distorted octahedral coordination environment, with four S atoms from two crystallographically nonequivalent  $ttp$  ligands acting in an asymmetric bischelating mode and two O atoms from the DMF ligands (Figure 1b). The

\* To whom correspondence should be addressed. E-mail: ptrikal@chemistry.uoc.gr.

<sup>†</sup> University of Crete.

<sup>‡</sup> Northwestern University.

(1) Robin, A. Y.; Fromm, K. M. *Coord. Chem. Rev.* **2006**, *250*, 2127.

(2) Janiak, C. *Dalton Trans.* **2003**, 2781–2804.

(3) (a) Rosi, N. L.; Eckert, J.; Eddaoudi, M.; Vodak, D. T.; Kim, J.; O’Keeffe, M.; Yaghi, O. M. *Science* **2003**, *300*, 1127–1129. (b) Chae, H. K.; Siberio-Perez, D. Y.; Kim, J.; Go, Y.; Eddaoudi, M.; Matzger, A. J.; O’Keeffe, M.; Yaghi, O. M. *Nature* **2004**, *427*, 523–527. (c) Park, K. S.; Ni, Z.; Cote, A. P.; Choi, J. Y.; Huang, R. D.; Uribe-Romo, F. J.; Chae, H. K.; O’Keeffe, M.; Yaghi, O. M. *Proc. Natl. Acad. Sci. U.S.A.* **2006**, *103*, 10186–10191. (d) Ferey, G.; Mellot-Draznieks, C.; Serre, C.; Millange, F. *Acc. Chem. Res.* **2005**, *38*, 217–225. (e) Kitagawa, S.; Kitaura, R.; Noro, S. *Angew. Chem., Int. Ed.* **2004**, *43*, 2334–2375. (f) Ferey, G.; Mellot-Draznieks, C.; Serre, C.; Millange, F.; Dutour, J.; Surble, S.; Margiolaki, I. *Science* **2005**, *309*, 2040–2042. (g) Liu, Y. L.; Kravtsov, V. C.; Larsen, R.; Eddaoudi, M. *Chem. Commun.* **2006**, 1488–1490. (h) Yaghi, O. M.; O’Keeffe, M.; Ockwig, N. W.; Chae, H. K.; Eddaoudi, M.; Kim, J. *Nature* **2003**, *423*, 705–714.

(4) (a) Xu, Z. *Coord. Chem. Rev.* **2006**, *250*, 2745–2757. (b) Li, K. H.; Xu, H. H.; Xu, Z. T.; Zeller, M.; Hunter, A. D. *Inorg. Chem.* **2005**, *44*, 8855–8860. (c) Zhong, J. C.; Misaki, Y.; Munakata, M.; Kuroda-Sowa, T.; Maekawa, M.; Suenaga, Y.; Konaka, H. *Inorg. Chem.* **2001**, *40*, 7096.

(5) Han, L.; Bu, X. H.; Zhang, Q. C.; Feng, P. Y. *Inorg. Chem.* **2006**, *45*, 5736–5738 and references cited therein.

(6) Mueller, U.; Schubert, M.; Teich, F.; Puetter, H.; Schierle-Arndt, K.; Pastre, J. J. *Mater. Chem.* **2006**, *16*, 626–636.

(7) Chisholm, M. H.; Patmore, N. J. *Dalton Trans.* **2006**, 3164–3169.

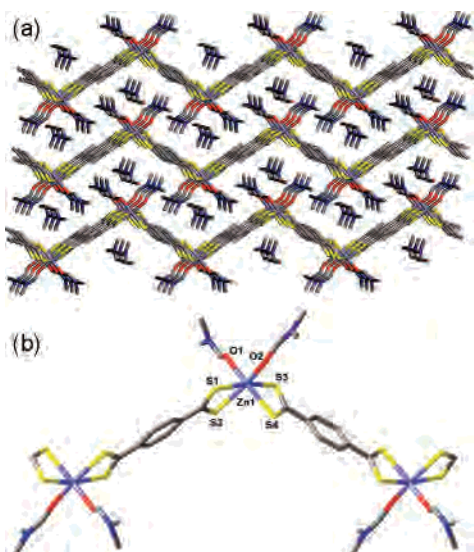


**Figure 1.** (a) Representative view of **1** looking approximately down the *a* axis. (b) Coordination environment of the Zn atoms in **1**. Selected crystallographic distances (Å) and angles (deg): Zn1–S1 2.430(2), Zn1–S2 2.648(2), S1–Zn1–S2 70.30(7), Zn1–S3 2.507(2), Zn1–S4 2.498(2), S3–Zn1–S4 71.45(7), Zn1–O1 2.134(5), Zn1–O2 2.057(6). H atoms are omitted for clarity.

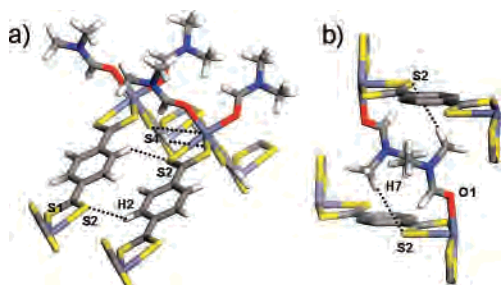


**Figure 2.** (a) Interchain C(sp<sup>2</sup>)–H···S hydrogen bonds in **1**. (b) Additional C(sp<sup>3</sup>)–H···S hydrogen bonds along the *b* axis between [<sub>∞</sub>Zn(S<sub>2</sub>CC<sub>6</sub>H<sub>4</sub>CS<sub>2</sub>)(DMF)<sub>2</sub>] chains from adjacent layers, exclusively via interdigitated DMF-1 molecules. Selected distances and angles: *d*<sub>C4–H2–S2</sub> = 2.864 Å, *θ*<sub>C4–H2–S2</sub> = 137.7°, and *φ*<sub>H2–S2–C1</sub> = 152.0° and *d*<sub>C10–H7–S2</sub> = 2.897 Å, *θ*<sub>C10–H7–S2</sub> = 159.0°, and *φ*<sub>H7–S2–C1</sub> = 87.4° (see ref 9).

[<sub>∞</sub>Zn(S<sub>2</sub>CC<sub>6</sub>H<sub>4</sub>CS<sub>2</sub>)(DMF)<sub>2</sub>] chains are running parallel and side by side along the [102] crystallographic direction and stack one on top of the other along the *b* axis. This arrangement reveals the existence of an extended two-dimensional (2D) network of C(sp<sup>2</sup>)–H···S hydrogen bonds<sup>9</sup> between adjacent chains and the formation of infinite supramolecular zigzag layers (see Figures 1a and 2a). The layers are packed efficiently via interdigitation of the coordinated DMF molecules along the *b* axis and held together by additional C(sp<sup>3</sup>)–H···S hydrogen bonds (Figure 2b). The resulting 3D supramolecular network features small cavities running along the *a* axis, in which noncoordinated DMF molecules reside (see Figure 1a). These molecules form relatively strong O···H–C hydrogen bonds with the coordinated DMF-1 molecules.

In the absence of any ionic interactions in **1**, the packing arrangement of the neutral [<sub>∞</sub>Zn(S<sub>2</sub>CC<sub>6</sub>H<sub>4</sub>CS<sub>2</sub>)(DMF)<sub>2</sub>] chains is clearly influenced by the C–H···S interactions between them. Moreover, the fact that **1** grows in the form of single crystals demonstrates their significant role in both directing and stabilizing the final structure. To the best of

our knowledge, **1** represents the first example of an extended, metal–organic solid in which C–H···S hydrogen bonds are essential elements in the crystal structure.<sup>9a</sup>

The synthesis of porous MOFs based on the BDC ligand relies on the formation of secondary building units (SBUs) through slow deprotonation of the acidic form of the ligand.<sup>10</sup> In contrast, when the anionic form of this ligand reacts directly with divalent metal ions such as Zn<sup>2+</sup>, no SBUs are formed and the products are nonporous 1D coordination polymers with 1:1 metal-to-ligand stoichiometry, similar to that of **1**.<sup>11</sup> Therefore, the instantaneous reaction between the ttp<sup>2-</sup> dianion and the labile Zn<sup>2+</sup> cations most likely prohibits the formation of an extended open-framework structure. It is important to note here that the ttp<sup>2-</sup> ligand is expected to form various types of SBUs similar to the molecular clusters that have been observed in the case of the dithiobenzoate ligand.<sup>12</sup> These clusters or SBUs are different from those obtained with carboxylate ligands because the S atom is larger than the O atom and, more importantly, because S has the ability to form three-coordinated sites. For these reasons, novel porous architectures may be accessible based on the SBU strategy, using a suitable precursor of the ttp ligand and appropriate synthetic conditions. It is noteworthy that a similar approach is not feasible in the case of aromatic thiolate ligands.<sup>5</sup>

Thermal gravimetric analysis (TGA) performed on a polycrystalline sample of **1** showed that the DMF molecules are completely removed in two distinct steps (Figure S3 in the Supporting Information). The first weight loss of 28.7% at 125 °C corresponds to the removal of two DMF molecules per formula unit (28.5% calculated) and the second of 14.0% at 180 °C to the removal of one DMF per formula unit (14.2% calculated). Interestingly, no weight loss was observed in the temperature range 180–300 °C, indicating the formation of a stable phase formulated as Zn(S<sub>2</sub>CC<sub>6</sub>H<sub>4</sub>CS<sub>2</sub>).<sup>13</sup> These results prompt us to investigate **1** further and especially to explore the chemistry associated with the labile DMF molecules. We found that when **1** is treated with CHCl<sub>3</sub> at room temperature, all DMF molecules are completely removed and the final solid, designated as **2**, contains no solvent molecules. This is confirmed by TGA and IR spect-

- (8) Single-crystal X-ray diffraction data: triclinic, space group *P* $\bar{1}$ , *a* = 7.0008(10) Å, *b* = 9.7164(11) Å, *c* = 16.693(2) Å, *α* = 94.219(10)°, *β* = 99.415(11)°, *γ* = 92.663(10)°, *V* = 1115.2(3) Å<sup>3</sup>, *Z* = 2, *ρ*<sub>calcd</sub> = 1.527 g/cm<sup>3</sup>, *T* = 100.0(3) K, 2 $\theta$  = 50.06°. Refinement of 253 parameters on 3204 independent reflections out of 14 818 measured reflections (*R*<sub>int</sub> = 0.1433) led to *R*<sub>1</sub> = 0.0724 [*I* > 2 $\sigma$ (*I*)], *wR*<sub>2</sub> = 0.1277 (all data), and *S* = 1.19 with the largest difference peak and hole of 0.60 and –0.54 e/Å<sup>3</sup>.
- (9) We have identified C–H···S hydrogen bonds using common criteria. These are the sum of the van der Waals radii for H and S (H, 1.20 Å; S, 1.80 Å) and the angles C–H···S (*θ*) and H···S–C (*φ*). See: (a) Cosp, A.; Larrosa, I.; Anglada, J. M.; Bofill, J. M.; Romea, P.; Urpi, F. *Org. Lett.* **2003**, *5*, 2809. (b) Novoa, J. J.; Rovira, M. C.; Rovira, C.; Veciana, J.; Tarres, J. *Adv. Mater.* **1995**, *7*, 233. (c) Bondi, A. J. *Phys. Chem.* **1964**, *68*, 441.
- (10) Li, H.; Eddaoudi, M.; O’Keeffe, M.; Yaghi, O. M. *Nature* **1999**, *402*, 276–279.
- (11) Guilera, G.; Steed, J. W. *Chem. Commun.* **1999**, 1563–1564.
- (12) Kano, N.; Kawashima, T. *Chalcogenocarboxylic Acid Derivatives. Topics in Current Chemistry*; Springer: Berlin, 2005; Vol. 251, pp 141–180.
- (13) No Bragg peaks were observed in the PXRD pattern of the solid obtained after heating **1** at 180 °C under an Ar flow.

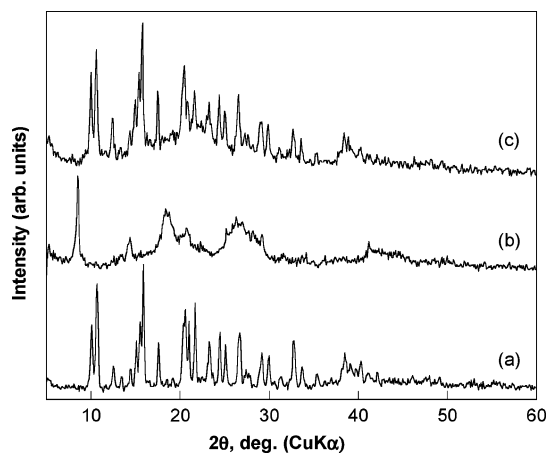


**Figure 3.** PXRD pattern (Cu  $K\alpha$  radiation) of (a) the as-made material **1**, (b) the corresponding solid **2** after DMF removal with  $\text{CHCl}_3$  treatment, and (c) the solid obtained after reintroduction of DMF.

roscopy (Figure S3 in the Supporting Information). Most surprising is the fact that **2** shows crystalline order, as evidenced by the diffraction lines observed in its powder X-ray diffraction (PXRD) pattern, albeit broadened and dissimilar to **1** (see Figure 3b). Remarkably, upon reintroduction of DMF, the solid exhibits the same PXRD pattern as **1**, as shown in Figure 3c. This facile and reversible removal of both coordinated and noncoordinated DMF molecules is quite impressive, especially if we take into account the fact that **1** is made of 1D chains held together only by  $\text{C-H}\cdots\text{S}$  hydrogen bonds, which usually are considered to be very weak with no clear role in the solid state.<sup>14</sup> It is entirely possible that in **2** the  $[\infty\text{Zn}(\text{S}_2\text{CC}_6\text{H}_4\text{CS}_2)]$  chains maintain their side-by-side  $\text{C-H}\cdots\text{S}$  hydrogen bonds (see Figure 2a) and the 2D supramolecular network is therefore susceptible to reversible removal of DMF molecules. In other words, **1** behaves like a layered material with intercalation properties.<sup>15</sup> Moreover, because this solid-to-solid-to-solid transformation involves only solvent molecules and occurs at room temperature, the structure of **2** should be closed to that of **1**. Therefore, it is highly unlikely that **2** is a collapsed version of **1**, but it most probably maintains an open architecture that is accessible by coordinating molecules.<sup>16</sup> A strong indication for the above arguments comes from the PXRD pattern of **2** (see Figure 3b), which shows a relatively strong Bragg peak in the low-angle region with a  $d$  spacing of 10.4 Å.

The reaction between the  $\text{ttp}^{2-}$  anions and  $\text{Mn}^{2+}$  under the same experimental conditions as those used in the synthesis of **1** leads to the formation of the isostructural compound  $[\text{Mn}(\text{S}_2\text{CC}_6\text{H}_4\text{CS}_2)(\text{DMF})_2](\text{DMF})$  as judged from its PXRD pattern and elemental analysis (Figure S6 in the Supporting Information). In addition, magnetic susceptibility measurement confirms the presence of  $\text{Mn}^{2+}$  (Figure S7 in the Supporting Information). However, in contrast to the Zn analogue, this material does not show a reversible removal of the DMF molecules.

The optical properties of the materials were investigated by solid-state diffuse-reflectance UV–vis/near-IR spectroscopy, and the results are shown in Figure 4. The free  $\text{ttp}^{2-}$  in the form of its dipiperidinium salt shows a well-defined optical absorption at 590 nm (2.10 eV) that originates from

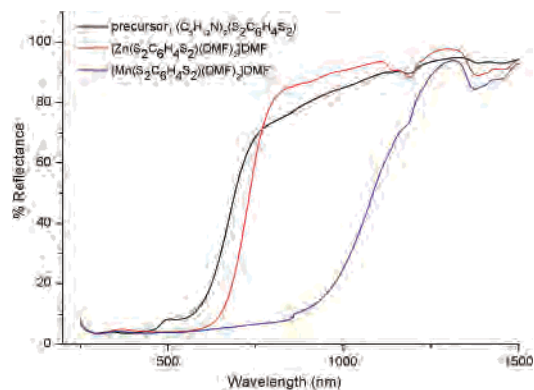


**Figure 4.** Solid-state UV–vis/near-IR diffuse-reflectance spectra of the precursor salt of the ligand and the corresponding coordination polymers recorded at room temperature.

the  $n \rightarrow \pi^*$  transition of the  $-\text{CSS}^-$  chromophore.<sup>17</sup> In contrast, the coordination polymers show optical absorptions that are clearly red-shifted and strongly depend on the nature of the transition metal. In the case of  $[\text{Mn}(\text{S}_2\text{CC}_6\text{H}_4\text{CS}_2)(\text{DMF})_2](\text{DMF})$ , the absorption occurs at 925 nm (1.34 eV), in accordance with its almost black color, while the isostructural Zn analogue (**1**), having dark-red color, absorbs at 660 nm (1.88 eV) (see Figure 4). The energies of these electronic transitions, which most likely originate from ligand-to-metal charge-transfer processes, are among the lowest that have been observed in the entire family of extended metal–organic networks, featuring no metal–metal bond, metal– $\pi$  interactions, or  $\pi$ – $\pi$  stacking.<sup>4</sup> A possible semiconductive behavior of these materials is currently under investigation.

In conclusion, the present work demonstrates that it is possible to construct crystalline coordination polymers based on the tetrathioterephthalate dianion as the bridging ligand. We anticipate that the two novel 1D  $[\text{M}(\text{S}_2\text{CC}_6\text{H}_4\text{CS}_2)(\text{DMF})_2](\text{DMF})$  ( $\text{M} = \text{Zn}, \text{Mn}$ ) compounds represent the first members of a new family of optoelectronically active metal–organic materials.

**Acknowledgment.** We are grateful to Prof. Mercurio G. Kanatzidis for providing the use of single-crystal XRD and solid-state diffuse-reflectance equipment. Financial support from the GSRT in Greece (PENED-03ED581) and Interreg IIIA (Gr-Cy, k2301.004) is gratefully acknowledged. We also thank Dr. Alexandros Lappas and Othon Adamopoulos at IESL-FORTH for the magnetic measurements.

**Supporting Information Available:** Instrumentation, experimental procedure, X-ray crystallographic file for **1** in CIF format, and additional characterization data. This material is available free of charge via the Internet at <http://pubs.acs.org>.

IC701414V

- (14) Bond, A. D.; Jones, W. J. *Chem. Soc., Dalton Trans.* **2001**, 3045.
- (15) When **2** is treated with something other than DMF coordinating molecules, such as pyridine and small alkylamines, new crystalline materials are formed. The corresponding PXRD patterns are provided in the Supporting Information. However, the atomic structures of these solids are currently unknown because the quality of the crystals does not allow single-crystal X-ray analysis.
- (16) A possible porosity in **2** was investigated by recording the nitrogen adsorption isotherm at 77 K. The results show that there is no permanent porosity, accessible at least by this probe molecule (see Figure S4 in the Supporting Information).
- (17) Furlani, C.; Luciani, M. L. *Inorg. Chem.* **1968**, *7*, 1586–1592.